5492 *Biochemistry* **2009,** *48,* 5492–5500
DOI: 10.1021/bi900261q

BIOCHEMISTRY
including biophysical chemistry & molecular biology
Article

A Thermodynamic Study of Ligand Binding to the First Three Domains of the Human Insulin Receptor: Relationship between the Receptor α-Chain C-Terminal Peptide and the Site 1 Insulin Mimetic Peptides[†]

John G. Menting, Colin W. Ward, Mai B. Margetts, and Michael C. Lawrence*

The Walter and Eliza Hall Institute of Medical Research, 1G Royal Parade, Parkville, Victoria 3052, Australia

Received February 17, 2009; Revised Manuscript Received April 23, 2009

ABSTRACT: The C-terminal segment of the insulin receptor (IR) α-chain plays a critical role in insulin binding. This 16-residue peptide together with the central β-sheet of the receptor L1 domain forms one of the insulin binding surfaces of the IR monomer. Here we use isothermal titration calorimetry to assay directly the binding of the IR αCT peptide to an IR construct (IR485) consisting of the three N-terminal domains of the receptor monomer. Our measurements show further that the binding of the IR αCT peptide to IR485 competes with the binding of a prototypical "Site 1" insulin mimetic peptide to the same receptor fragment. The competitive nature of their binding appears to be reflected in a previously undetected sequence similarity between the IR αCT peptide and the Site 1 mimetic peptide. In contrast, a prototypical "Site 2" peptide has very limited affinity for IR485. Taken together, these results complement our recent observation that there is a possible structural relationship between these mimetic peptides and insulin itself. They also add support to the view that the segment of unexplained electron density lying on the surface of the central β-sheet of the L1 domain in the IR ectodomain crystal structure arises from the IR αCT peptide. Finally, we show that mutation of the critical IR αCT peptide residue Phe714 to alanine does not affect the peptide's affinity for IR485 and conclude that the resultant loss of insulin binding with this mutation results from loss of interaction of the phenylalanine side chain with insulin.

The human insulin receptor (IR)[1], the type 1 insulin-like growth factor receptor (IGF-1R), and the insulin receptor-related receptor (IRR) form a homologous family of homodimeric $\alpha_2\beta_2$ receptor tyrosine kinases (*1*). Insulin binding to the IR displays complicated kinetics, consistent with the existence of both low- and high-affinity states as well as negative cooperativity (*2*, *3*). Little is known about these events at the atomic level of detail. The current model of insulin binding to receptor postulates that each IR αβ monomer contains two distinct ligand-binding regions (termed Site 1 and Site 2 in one monomer and Site 1′ and Site 2′ in the other) and also that insulin itself contains two receptor binding surfaces. Low-affinity binding occurs when insulin binds via one surface to Site 1 on one IR monomer, which is then followed by a high-affinity cross-linking of insulin via its second surface to Site 2′ on the other IR monomer. Within this model, negative cooperativity results from subsequent ligand binding to the alternate Site 1′−Site 2 pair and the concomitant reduction in affinity at the initial Site 1−Site 2′ pair. A major advance was the recent determination of the crystal structure of the IR ectodomain in its apo form (*4*), which revealed that the constituent domains are arranged in a 2-fold symmetric, inverted "V" conformation. Each leg of the inverted V is formed by the first leucine-rich repeat domain (L1), the cysteine-rich region (CR), and the second leucine-rich repeat domain (L2) of one receptor monomer juxtaposed against the three fibronectin type III domains (FnIII-1, -2, and -3) of the alternate receptor monomer. FnIII-2 has within its CC′ loop the ∼120-residue insert domain (ID), which contains the α/β cleavage site. The ID is largely disordered within the crystal structure, consistent with early predictions that it is indeed largely devoid of secondary structure (*5*). The ectodomain crystal structure revealed that the surface of the central β-sheet of the L1 domain, which forms part of Site 1 (*6*), lies in the proximity of loops at the junction of FnIII-1 and FnIII-2 of the opposite monomer, implicating these elements in the formation of Site 2. This conclusion is consistent with earlier studies of receptor chimeras (*7*−*9*) and has since been functionally confirmed by alanine scanning mutagenesis (*10*).

[†]This work was supported by Australian National Health and Medical Research Council (NHMRC) Grant 516729, NHMRC Independent Research Institutes Infrastructure Support Scheme Grant 361646, and a Victorian State Government Operational Infrastructure Support Grant.

*To whom correspondence should be addressed. Telephone: +61393452693. Fax: +61393452686. E-mail: lawrence@wehi.edu.au.

[1]Abbreviations: CR, cysteine-rich region; $\Delta H°$, observed enthalpy of binding; $\Delta S°$, observed entropy of association; DLS, dynamic light scattering; FnIII, fibronectin type III domain; ID, insert domain; IGF-1R, type 1 insulin-like growth factor receptor; IGF-I, insulin-like growth factor-I; IR, insulin receptor; αCT, 16-residue C-terminal segment of the IR or IGF-1R α-chain; IRR, insulin receptor-related receptor; ITC, isothermal titration calorimetry; K_d, dissociation constant; L1, first leucine-rich repeat domain; L2, second leucine-rich repeat domain; NMR, nuclear magnetic resonance; TBSA, Tris-buffered saline with 0.02% azide; ZFP-insulin, zinc-free porcine insulin.

Published on Web 05/21/2009

Intriguingly, the IR ectodomain crystal structure exhibited a tube-like segment of electron density lying across the central β-sheet of both L1 domains (*4*, *11*). It was proposed that this electron density feature arose at least in part from the C-terminal region of the receptor α-chain as this region (termed the IR αCT peptide) is known to play a critical role in ligand binding (*12*, *13*). Evidence of such a role arises from the observation that addition of either exogenous or covalently attached IR αCT peptide imparts nanomolar insulin binding to an IR construct consisting solely of the first three domains of the receptor (IR468), which is otherwise devoid of ligand binding ability (*14*−*17*). Additional evidence of the involvement of the IR αCT peptide in insulin binding comes from photo-cross-linking studies, which show that insulin residues B25, A3, and A8 can be cross-linked to the IR αCT peptide (*12*, *18*, *19*).

To explore the role of the IR αCT peptide further, we have used isothermal titration calorimetry (ITC) to assay directly the interactions between the IR αCT peptide and IR485 (a construct also consisting of the first three domains of the IR, but slightly longer than IR468), as well as the interaction between the analogous peptide of human IGF-1R and IR485. IR485 is known to dimerize through its ligand binding surfaces at high concentrations (*6*), and we have thus also sought to monitor the multimeric state of IR485 in the presence of ligand using dynamic light scattering (DLS). Our ITC studies also include an examination of the thermodynamics of binding of the N- and C-terminal segments of the insulin mimetic peptide S519 (*20*) to IR485, as well as the binding of S519 itself to IR485. S519 is a 36-residue peptide resulting from the affinity optimization of two covalently linked peptides, S371, a so-called "Site 1" peptide, and S446, a so-called "Site 2" peptide (*21*).[2] S519 binds human IR with a K_d of 2.0×10^{-11} M (*20*). Taken together, our results reveal a remarkable relationship between the IR αCT peptide and the Site 1 mimetic peptide, complementing our recent observation of possible structural similarity between the mimetic peptides and insulin itself (*22*). Finally, we have examined the binding to IR485 of the IR αCT peptide carrying a F714A mutation, a modification known to reduce the affinity of the receptor for insulin (*13*, *17*).

MATERIALS AND METHODS

Reagents. The IR485 construct of human IR was expressed in Lec8 mutant CHO cells and purified by gel filtration chromatography as described previously (*6*). All mammalian cell culture was performed under contract by the fermentation group of CSIRO Molecular and Health Technologies. IR485 consists of the first 485 residues of the mature human insulin receptor followed by the 17-residue sequence SDDDDKEQKLISEEDLN, which comprises a serine residue followed by an enterokinase cleavage site and a c-myc epitope tag. The c-myc tag was not removed for the ITC studies described here. IR485 was concentrated to 30 mg/mL in Tris-buffered saline (TBSA) [24.8 mM Tris-HCl (pH 8.0), 137 mM NaCl, 2.7 mM KCl, and 0.02% sodium azide] using an Ultrafree centrifugal concentrator (Millipore). Porcine insulin (Sigma-Aldrich) was prepared in a zinc-free form (termed ZFP-insulin) by extensive dialysis against 0.1% (v/v) acetic acid followed by lyophilization. Human IGF-I was obtained from Novozymes GroPep as "receptor grade" material. The IR αCT peptide (residues 704−719, TFEDYLHNVVFVPRPS), the IGF-1R αCT peptide (residues 691−706, VFENFLHNSIFVPRPE), and the F714A mutant of IR αCT (denoted IR-CT.714A) were obtained from Genscript Corp. at the >98% level of purity. The S519N20 peptide (SLEEEWAQVECEVYGRGCPS) and the S519C16 peptide (GSLDESFYDWFERQLG) were obtained from AusPep at the >90% level of purity. The S519 peptide (SLEEEWAQVECEVYGRGCPSGSLDESFYDWFERQLG) was obtained from Activotec at the >85% level of purity. Peptides were dissolved in 10 mM HCl at a concentration of ~4 mg/mL and then diluted with TBSA. Oxidation of peptides S519N20 and S519 (which contain two cysteine residues) was carried out by incubating the respective peptide (prepared at 1 mg/mL in 50 mM ammonium bicarbonate adjusted to pH 8.5 with an ammonia solution) in the dark at room temperature for 2 days and then lyophilizing before use. Oxidation was complete as determined by analysis with Ellman's reagent [5,5′-dithiobis(2-nitrobenzoate) (*23*, *24*)]. All protein concentrations were determined by absorbance measurement at 280 nm using a NanoDrop 1000 spectrophotometer (Thermo Scientific).

Isothermal Titration Calorimetry. ITC experiments were performed using a VP-ITC isothermal titration calorimeter (MicroCal Inc.) with the calorimeter cell held at 25 °C. All samples were degassed prior to injection or placement into the cell, and the instrument was temperature-equilibrated prior to the start of the injections. In all experiments, the volume of the sample placed in the cell was 1.4 mL and the titrant was injected in 7 μL volumes over 14 s at 3 min intervals, with the total number of injections being 40. The sample contents were stirred at a speed of 310 rpm over the duration of the titration. All titrants (i.e., ZFP-insulin, IGF-I, IR αCT peptide, IGF-1R αCT peptide, IR αCT.714A peptide, S519, S519N20, and S519C20) were first injected into a solution of TBSA alone to ascertain the heat of dilution, which was then subtracted from the data of interest as appropriate. Data were analyzed using the instrument's software incorporated within Origin 7 (OriginLab) and in all cases fitted as a single-site interaction using the methodologies outlined in the instrument's manual. All measurements showing quantifiable interaction were conducted in triplicate (in some cases at varying concentrations) and the resultant ITC-derived thermodynamic parameters averaged.

Dynamic Light Scattering. DLS measurements were conducted using a Zetasizer NanoZS (Malvern Instruments Ltd.). Samples of IR485 and IR485 in combination with IR αCT and/or ZFP-insulin at various concentrations were prepared in TBSA and equilibrated overnight at 4 °C. Samples were spun at 13000*g* using a benchtop centrifuge to pellet any macroscopic particulates and then pipetted into a 45 μL glass cuvette held at 20 °C. Data were analyzed using the instrument's Dispersion Technology Software version 5.0.2 to yield a volume distribution for the scattering particles present in the solution. The results presented are representative of several sets of experiments.

RESULTS

Pairwise Interactions of IR485, Hormones, and αCT Peptides. Our first set of ITC experiments investigated the pairwise interaction between selected combinations of IR485, ZFP-insulin, IGF-I, IR αCT peptide, IGF-1R αCT peptide, and IR αCT.714A peptide. The results of the analyses are listed in Table 1. The mean dissociation constants (K_d) of the interaction

[2]Note that the Site 1 and Site 2 nomenclature used for the insulin mimetic peptides is based on their grouping according to competition (*21*) and is a priori unrelated to the Site 1 and Site 2 nomenclature used for the two binding surfaces for insulin upon the receptor.

Table 1: ITC Analysis of Pairwise Interactions of IR485, Hormone, and αCT Peptides[a]

sample	[sample] (μM)	titrant	[titrant] (μM)	K_d (μM)
ZFP-insulin	20	IR αCT	200	≳1000
IGF-I	20	IGF-1R αCT	200	≳1000
IR485	5	ZFP-insulin	50	≳1000
IR485	10	IGF-I	100	≳1000
IR485	10	IR αCT	60	3.3 ± 1.1
IR485	20	IGF-1R αCT	120−150[b]	17.6 ± 2.1
IR485	10	IR αCT.714A	60	6.5 ± 1.7

[a] K_d values are of the means of three experiments with each set of experimental data being modeled as a single-site interaction between the titrant and sample (see Materials and Methods). The error stated is the standard error of the mean. The relatively low value of the Wiseman parameter c coupled with the noise in the data precludes accurate determination of $\Delta H°$ (and hence of $T\Delta S°$). [b] Ranges are quoted for a sample or titrant concentration where these vary across the three measurements.

between (i) IR αCT and IR485, (ii) IGF-1R αCT and IR 485, and (iii) IR αCT.714A and IR485 were determined to be 3.3 ± 1.1, 17.6 ± 2.1, and 6.5 ± 1.7 μM, respectively. Representative ITC profiles for these measurements are presented in Figure 1. The dissociation constant (K_d) for the interactions between (i) ZFP-insulin and IR αCT peptide, (ii) IGF-I and IGF-1R αCT peptide, (iii) ZFP-insulin and IR485, and (iv) IGF-I and IR485 was in all cases estimated to be weaker than 1 mM.

Interaction of the Hormone with IR485 Precomplexed with αCT Peptides. Our second set of ITC experiments investigated the interaction of ZFP-insulin and IGF-I with IR485 precomplexed with a 10-fold molar ratio of either IR αCT, IR αCT.714A, or IGF-1R αCT peptide. Given that these peptides display micromolar affinity for IR485 (see above), we calculate that, at the concentrations of IR485 and αCT peptide employed in this set of experiments, ≥90% of the IR485 molecules within the ITC cell are in complex with αCT peptide prior to injection of hormone. The results of the ITC investigations are presented in Table 2 with representative ITC curves being presented in Figure 2. The dissociation constant of ZFP-insulin with respect to IR485 in the presence of a 10-fold molar ratio of IR αCT peptide is 17 ± 4 nM and in the presence of a 10-fold molar ratio of IGF-1R αCT peptide is 5.7 ± 1.1 nM. In contrast, the dissociation constant of IGF-I with respect to IR485 in the presence of a 10-fold excess of IR αCT peptide is 490 ± 75 nM and in the presence of a 10-fold excess of IGF-1R αCT peptide is 22 ± 3 nM, with no correction being made for the incomplete saturation of IR485 with peptide prior to injection. The thermodynamic parameters listed in Table 2 show that in all four of these cases the binding of hormone to αCT peptide precomplexed with IR485 is enthalpically driven. No binding could be detected for insulin titrated against IR485 precomplexed with IR αCT.714A, with the K_d being estimated to be weaker than 1 mM (ITC traces not shown).

Interaction of Insulin Mimetic Peptides with IR485. Our third set of ITC experiments investigated the interaction of the insulin mimetic peptides S519, S519N20 (a Site 2 peptide, corresponding to the 20 N-terminal residues of S519), and S519C16 (a Site 1 peptide, corresponding to the 16 C-terminal residues of S519) with IR485. The results are presented in Table 3, with representative ITC curves being presented in Figure 3. S519 binds IR485 with a dissociation constant of 11 ± 3 nM, while S519C16 binds IR485 with a somewhat higher affinity (K_d =

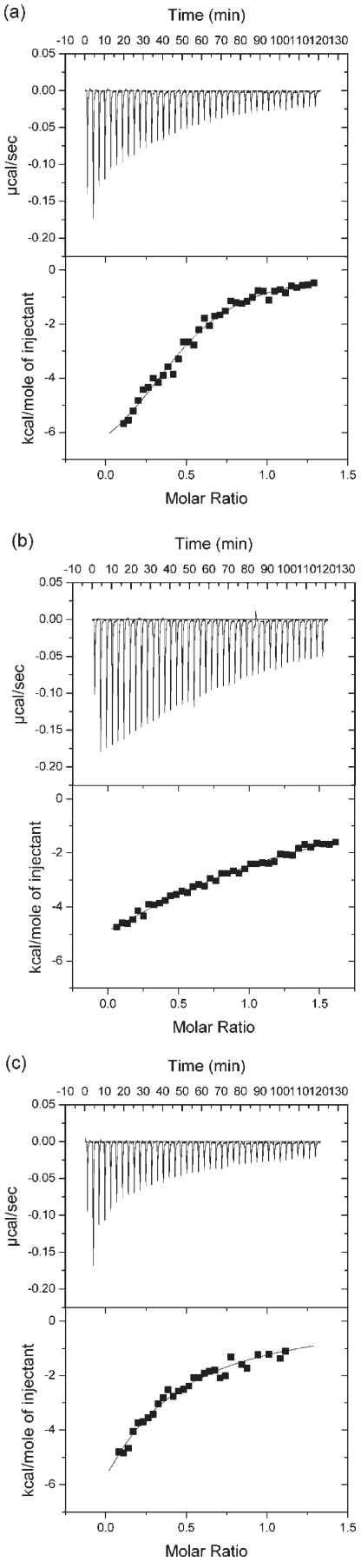

FIGURE 1: ITC curves for the titration of (a) IR αCT peptide against IR485, (b) IGF-1R αCT peptide against IR485, and (c) IR αCT.714A peptide against IR485.

Table 2: Isothermal Titration of ZFP-Insulin and IGF-I against IR485 Premixed with a 10-fold Molar Ratio of either IR or IGF-1R αCT Peptide[a]

sample	[sample] (μM)	titrant	[titrant] (μM)	K_d (nM)	$\Delta H°$ (kJ/mol)	$-T\Delta S°$ (kJ/mol)
IR485 with 10× IR αCT	5	ZFP-insulin	50	17 ± 4	−67 ± 1	22 ± 2
IR485 with 10× IGF-1R αCT	4−10[b]	ZFP-insulin	32−60	5.7 ± 1.1	−97 ± 2	50 ± 2
IR485 with 10× IR αCT	5−10	IGF-I	50−80	490 ± 75	−89 ± 2	53 ± 2
IR485 with 10× IGF-1R αCT	4−5	IGF-I	40−50	22 ± 3	−101 ± 1	57 ± 1
IR485 with 10× IR αCT.714A	5	ZFP-insulin	50	≳1 mM		[c]

[a] K_d, $\Delta H°$, and $T\Delta S°$ values are the means of three experiments with each set of experimental data being modeled as a single-site interaction between titrant and sample (see Materials and Methods). The error stated is the standard error of the mean. [b] Ranges are quoted for sample or titrant concentration where these vary across the three measurements. [c] The affinity of the interaction is too too weak to allow meaningful calculation of either $\Delta H°$ or $T\Delta S°$.

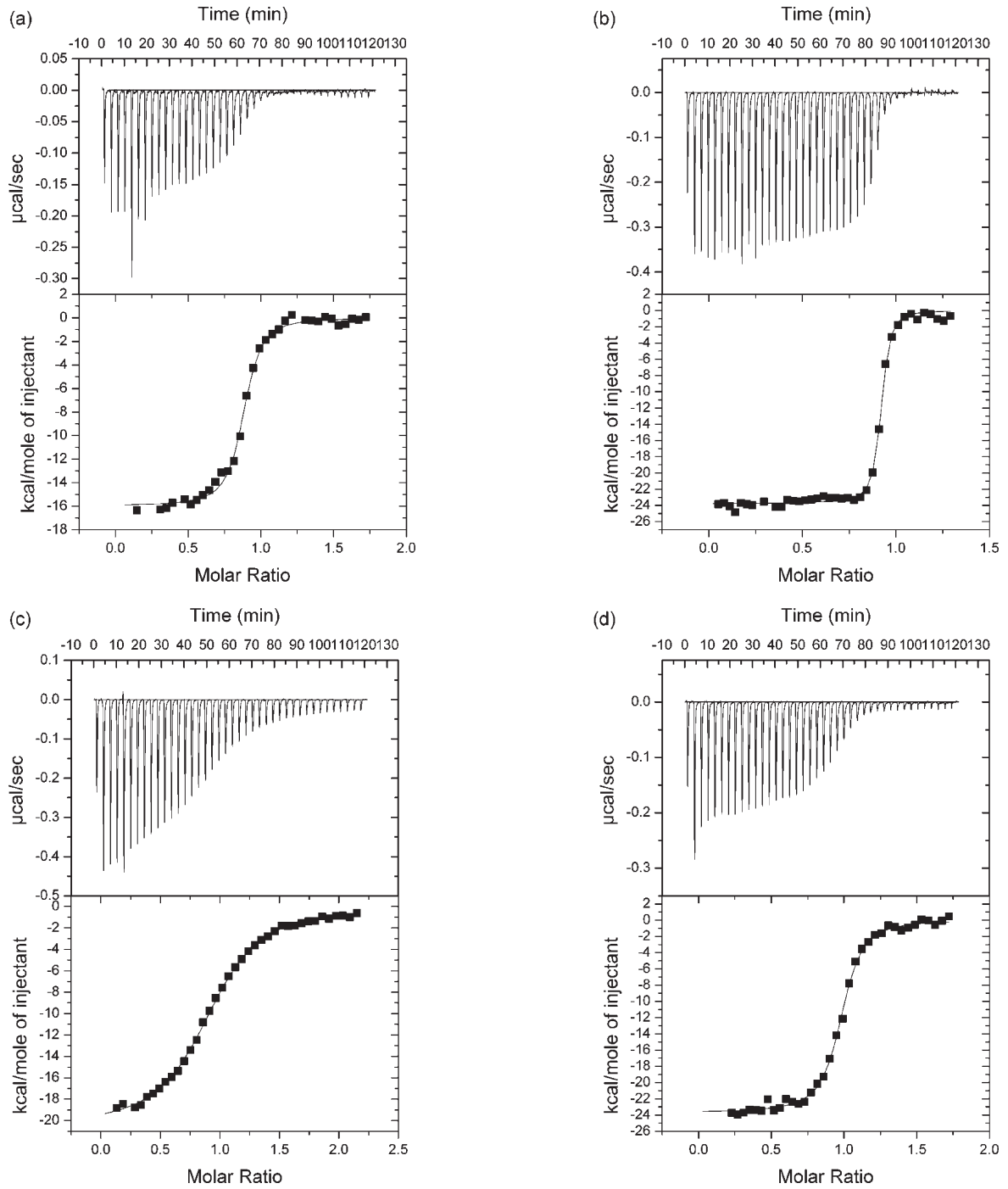

FIGURE 2: ITC curves for the titration of (a) ZFP-insulin against IR485 precomplexed with a 10-fold molar ratio of IR αCT peptide, (b) ZFP-insulin against IR485 precomplexed with a 10-fold molar ratio of IGF-1R αCT peptide, (c) IGF-I against IR485 precomplexed with a 10-fold molar ratio of IR αCT peptide, and (d) IGF-I against IR485 precomplexed with a 10-fold molar ratio of IGF-1R αCT peptide.

Table 3: Isothermal Titration of Insulin Mimetic Peptides S519, S519N20, and S519C16 against IR485[a]

sample	[sample] (μM)	titrant	[titrant] (μM)	K_d (nM)	$\Delta H°$ (kJ/mol)	$-T\Delta S°$ (kJ/mol)
IR485	4.5−5[b]	S519	40−50	11 ± 3	−69 ± 6	24 ± 6
IR485	5	S519C16	50	2.6 ± 0.7	−61 ± 4	12 ± 4
IR485 with 10× IR αCT	3−5	S519C16	45−50	16 ± 6	−33 ± 2	−11 ± 3
IR485	5	S519N20	50	≳1 mM	[c]	

[a] K_d, $\Delta H°$, and $T\Delta S°$ values are the means of three experiments with each set of experimental data being modeled as a single-site interaction between titrant and sample (see Materials and Methods). The error stated is the standard error of the mean. [b] Ranges are quoted for sample or titrant concentration where these vary across the three measurements. [c] The affinity for the interaction of S519N20 with IR485 is too weak to allow meaningful calculation of either $\Delta H°$ or $T\Delta S°$.

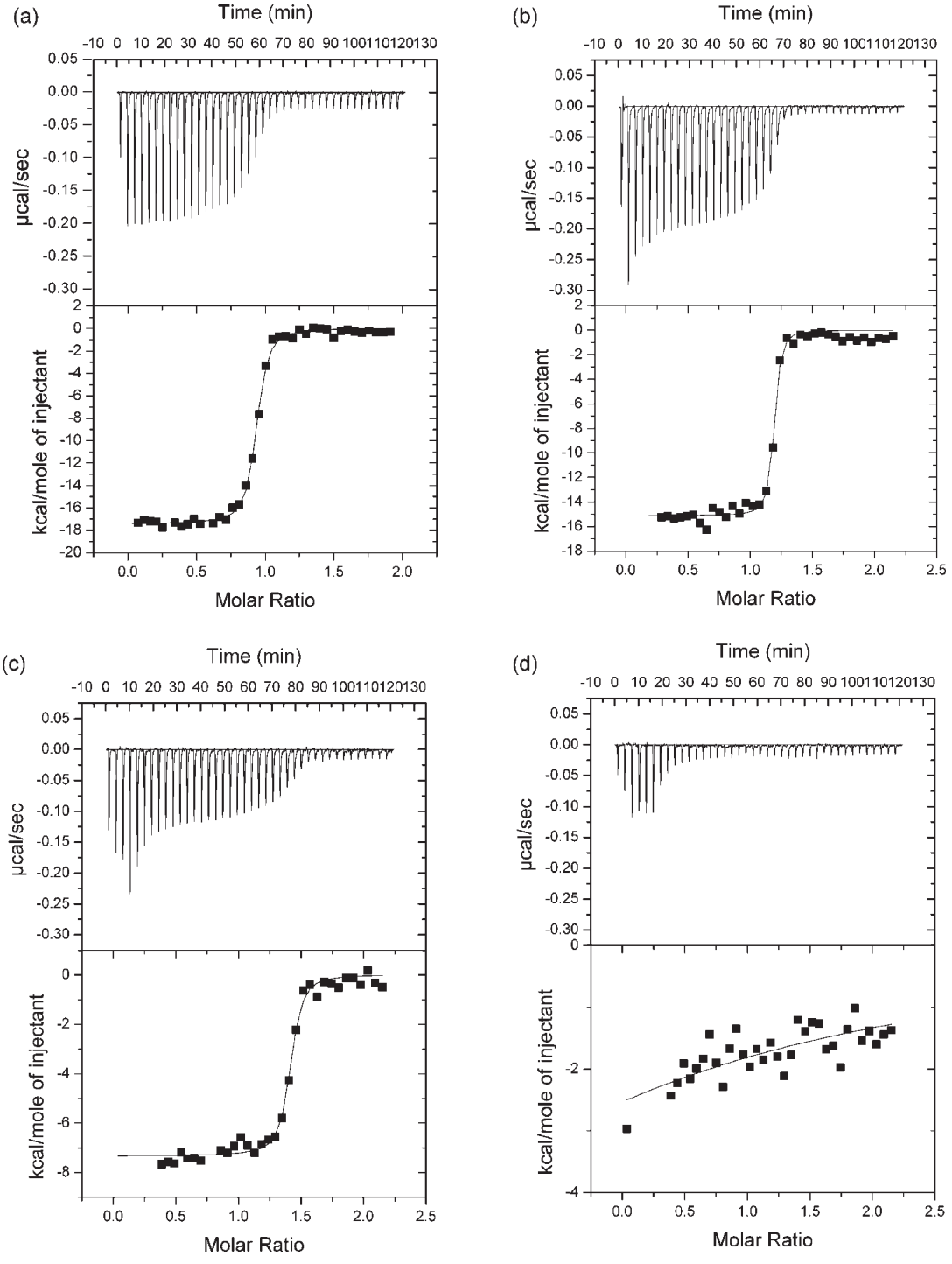

FIGURE 3: ITC curves for the titration of (a) S519 against IR485, (b) S519C16 against IR485, (c) S519C16 against IR485 precomplexed with a 10-fold molar ratio of IR αCT peptide, and (d) S519N20 against IR485.

2.6 ± 0.7 nM). The binding of both S519 and S519C16 to IR485 appears to be enthalpically driven. When IR485 is in the presence of a 10-fold molar ratio of IR αCT peptide, the dissociation constant for S519C16 increases to 16 ± 6 nM. The dissociation constant for the interaction between S519N20 and IR485 is estimated to be weaker than 1 mM, with accurate determination of K_d precluded at the concentrations of reactants employed.

Multimeric State of IR485 in the Presence of IR αCT Peptide. The DLS-determined volume distribution of IR485 at 6 mg/mL [a concentration at which IR485 is overwhelmingly dimeric (*6*)] shows a single broad peak centered at a particle diameter of 9.7 nm (Figure 4a). The half-width of the peak is 3.1 nm and the assumption of a spherical particle lead to a calculated scattering particle molecular mass of 136 kDa, closely similar to the molecular mass of ~140 kDa estimated by size-exclusion chromatography. Instrumental limitations preclude DLS measurement of IR485 at concentrations at which IR485 is known to be overwhelmingly monomeric [i.e., at < 0.025 mg/mL (*6*)]. However, at 0.5 mg/mL, the DLS-determined volume distribution of IR485 shows a single broad peak at a particle diameter of 8.2 nm (Figure 4b). The half-width of the peak is 2.2 nm, and the assumption that the scattering arises from a single species of spherical scattering particle leads to a calculated molecular mass of 91 kDa, consistent with the solution being predominantly monomeric. Using this pair of observations as reference values, we then observe that (i) an addition of a 3-fold molar ratio of

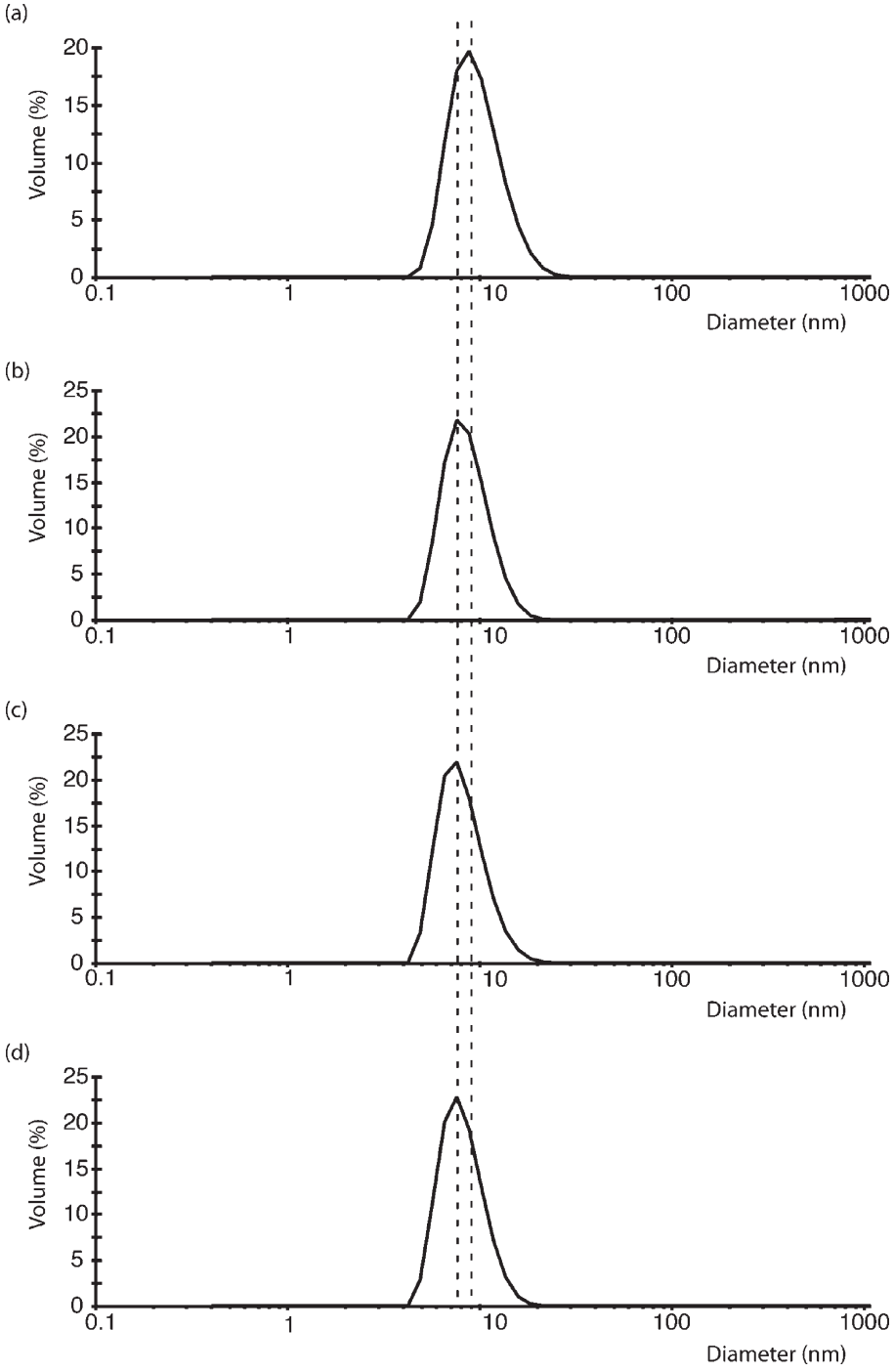

FIGURE 4: Dynamic light scattering volume distribution curves obtained from samples of (a) IR485 at 6 mg/mL, (b) IR485 at 0.5 mg/mL, (c) IR485 at 6 mg/mL with a 3-fold molar ratio of IR αCT peptide, and (d) IR485 at 6 mg/mL with a 3-fold molar ratio of IR αCT peptide and a 2-fold molar ratio of ZFP-insulin.

IR αCT peptide to a 6 mg/mL solution of IR485 results in a DLS-determined volume distribution which has a single peak centered at 8.6 nm (Figure 4c) and (ii) an addition of a 3-fold molar ratio of IR αCT peptide together with a 2-fold molar ratio of ZFP-insulin to a 6 mg/mL solution of IR485 results in a volume distribution which has a single peak centered at 8.2 nm (Figure 4d). The half-width of these latter two peaks is 2.4 nm, and the calculated molecular masses of the scattering particles (again assuming a single species of spherical scatterers) are 102 and 92 kDa, respectively. These data imply that addition of either (i) IR αCT peptide or (ii) IR αCT peptide with ZFP-insulin to a 6 mg/mL solution of IR485 results in a change in its hydrodynamic diameter consistent with the construct undergoing a transition from being overwhelmingly dimeric in solution to predominantly monomeric in solution.

DISCUSSION

We believe this study to be the first ITC investigation of ligand binding to the insulin receptor ectodomain or fragments thereof. ITC has the advantage of measuring the binding equilibrium directly by determining the heat evolved on association of a ligand with its receptor, which in turn leads to direct calculation of the enthalpy of binding ($\Delta H°$) and the dissociation constant (K_d). Furthermore, ITC does not require modification of the ligand (as is the case with assays based on the radiolabeling or europium labeling of ligand), nor does it require capture of either interactant on a substrate (as is the case with surface plasmon resonance measurement or assays utilizing antibody capture). The drawback is that ITC utilizes a considerably higher quantity of protein than other techniques. In this study, we have exploited methodologies that we developed earlier to generate IR485 in milligram amounts (*6*) to produce quantities suitable for ITC analysis. Even so, in the case of measurements of the micromolar-affinity interaction of the IR αCT peptide and IR485, restriction on the availability of protein required us to limit our calorimetry to a regime in which the Wiseman parameter, c [the product of the initial receptor concentration within the calorimetry cell and the association constant, K_a (*25*)], is approximately unity. Although the c value of $\approx$1 is lower than that normally recommended for ITC studies (i.e., $c \gtrsim 10$), we point out that it is now accepted that ITC can be conducted at considerably lower values of c (*26*), even down to c values on the order of 10^{-4} (*27*) with appropriate experimental design.

It has been shown (*17*) that it is possible to restore nanomolar insulin binding to the monomeric receptor construct IR468 (which consists of the L1, CR, and L2 domains of IR) by the addition of an excess of exogenous IR αCT peptide to the construct in solution. This result led to the inference (*17*) that the αCT peptide has a low micromolar affinity for IR468. Our data now, for the first time, demonstrate directly such an interaction (Table 1), using the IR αCT peptide and a closely similar receptor construct (IR485). A similar micromolar affinity is demonstrated between IR485 and the IGF-1R αCT peptide. Our data also confirm (Table 2) the earlier observations (*17*) that (i) addition of an excess of the αCT peptide of either IR or IGF-1R to a construct consisting of the first three domains of IR enables the construct to bind insulin with nanomolar affinity and (ii) the affinity of the construct for insulin in the presence of the IGF-1R αCT peptide is somewhat greater than that in the presence of the IR αCT peptide. Our ITC experiments also extend these observations and show that an IR construct consisting of the first three domains of the receptor also binds IGF-I with nanomolar affinity in the presence of an excess of the IGF-1R αCT peptide (Table 2). However, the affinity of IR485 for IGF-I in the presence of an excess of the IR αCT peptide is considerably lower ($K_d = 490 \pm 75$ nM). The higher affinity of IR485 for IGF-I in the presence of excess IGF-1R αCT peptide as compared to that in the presence of IR αCT peptide is consistent with the alanine scanning mutagenesis results which show that the IGF-1R αCT peptide is the most important contributor to IGF-I binding (*28*).

We now consider the tube of electron density observed on the surface of the central β-sheet of the L1 domain in the X-ray crystal structure of the IR-A ectodomain (*4*). Our findings here confirm that this segment of density almost certainly does not arise from the Site 2 S519N20 peptide that was present in the crystallization mother liquor, as the affinity of IR485 for this peptide is very low. However, it is not immediately clear that the density is associated with ordered IR αCT peptide, as the interaction observed here between IR αCT peptide and IR485 may be at a different site on the construct surface. To address this issue further, we have investigated the self-association of IR485, which is known to be predominantly dimeric at concentrations greater than approximately 0.8 mg/mL (*6*). We surmise that this self-association is mediated by central β-sheets of the L1 domains, given that pairs of adjacent IR485 molecules within the crystal structure (*6*) are observed to have an extensive pseudosymmetric interaction of these elements, with all other crystal contacts being sparse. Hence, if the tube of electron density observed on the equivalent L1 central β-sheet surface in the IR ectodomain crystal structure does indeed arise from bound IR αCT peptide, then we would reasonably expect the IR αCT peptide to be capable of disrupting the self-dimerization of IR485. Our DLS data (Figure 4) show this to be the case: addition of either IR αCT peptide or IR αCT peptide with ZFP-insulin to a solution of IR485 at 6 mg/mL results in a reduction in its hydrodynamic diameter from a value consistent with the dimeric species to a value that is consistent with a predominantly monomeric species of the construct. Taken together, our ITC and DLS data thus lend very strong support to the argument that the electron density feature on the surface of the central β-sheet of the L1 domain arises from the ordered IR αCT peptide.

We have shown that the Site 1 insulin mimetic peptide S519C16 binds to IR485 with nanomolar affinity and that this affinity is reduced by approximately 5-fold in the presence of the IR αCT peptide (Table 3). A statistical t test shows that this reduction is significant at the 95% level of confidence. We note that $-T\Delta S°$ is negative when S519C16 is titrated against IR485 in the presence of IR αCT peptide (Table 3), as opposed to being positive when the titration is performed in the absence of IR αCT peptide. Taken together, these data imply that S519C16 peptide and IR αCT peptide bind IR485 competitively. The increase in entropy associated with the release of the IR αCT peptide in the presence of the S519C16 peptide may arise in part with a loss of secondary structure of IR αCT peptide, as we note that nuclear magnetic resonance measurements show that IR αCT has a random coil conformation in solution (R. Norton and C. Galea, personal communication).

Do the Site 1 insulin mimetic peptide S519C16 and the IR αCT peptide target the same site or overlapping sites on sIR485? In this regard, we point out (Figure 5) the fact that there is an intriguing level of sequence identity between the Site 1 mimetic

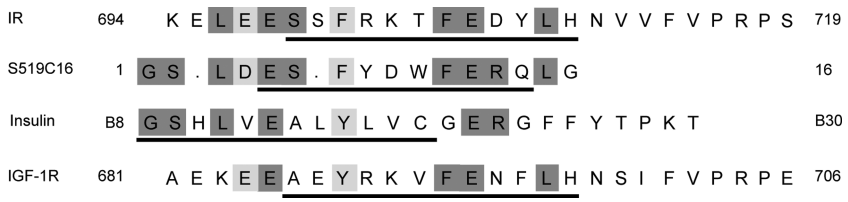

FIGURE 5: Sequence alignment of the C-terminal segment of the IR-A α-chain (IR-A numbering), the C-terminal segment of the IGF-1R α-chain, the 16 C-terminal residues of the insulin mimetic peptide S519, and the insulin B-chain. Underlined segments correspond to those either known to have a helical conformation (in the case of insulin) or predicted to have helical propensity [in the case of the remaining peptides (*22*)]. Shading indicates discerned sequence similarity across the helical segments (dark gray for identical residues and light gray for conservative substitution).

peptide S519C16 and residues 696−709 of the insulin receptor, a region that overlaps with that of the αCT peptide. In particular, we note in this alignment the correspondence of IR residues Phe701 and Phe705 with S519C16 residues Phe7 and Phe11, respectively; these latter two residues form part of the so-called "Motif 1" of the Site 1 mimetic peptides (*21*). This relationship between the IR αCT peptide and S519C16 is tantalizingly similar to the sequence identity (Figure 5) that S519C16 shares with the B-chain of insulin (*22*). The putative relationship among these respective regions of the IR insert domain, the B-chain of human insulin, and the S519C16 mimetic peptide is supported by the fact that these peptides either are known to be helical in structure or are predicted to have helix forming propensity (*22*). We thus speculate that on their respective binding to IR, both the B-chain helix of insulin and the Site 1 insulin mimetic peptide S519C16 occupy a site on the surface of the central β-sheet of L1 closely similar to that occupied by the IR αCT peptide in the apo receptor. However, in the case of insulin binding, cross-linking data (*12*, *18*, *19*) imply that, in the intact receptor, the IR αCT peptide segment remains in association with both the hormone and the receptor.

The full-length S519 mimetic peptide binds IR485 with a nanomolar affinity closely similar to that of its C-terminal (Site 1) fragment (Table 3). This stands in contrast to its affinity for the whole receptor, which is approximately 2 orders of magnitude greater (*20*). Our data imply that this additional affinity likely results from an interaction between the N-terminal (Site 2) fragment of the peptide and regions of the receptor ectodomain distinct from the L1−CR−L2 fragment. It has been suggested that the covalently linked Site 1−Site 2 or Site 2−Site 1 mimetic peptides have a sandwich structure similar to that of insulin (*22*). Within this model, S519N20 would mimic the A-chain of insulin and likely form interactions with residues at the junction of the FnIII-1 and FnIII-2 domains.

Finally, we have measured the affinity of the IR αCT.714A peptide for the IR485 construct (Table 1). Phe714 has been implicated as a key residue in the αCT peptide−ligand−receptor interaction, as it is the only residue within the IR αCT peptide that is (a) conserved in IGF-1R, (b) not conserved within IRR (*16*), and (c) intolerant of alanine substitution in mutagenesis studies of ligand binding to the chimeric minireceptors (*17*) and soluble IR ectodomains (*13*). We have shown here that the IR αCT.714A peptide binds IR485 with an affinity closely similar to that of the native IR αCT peptide, while the F714A mutation, as anticipated (*17*), abrogates binding of ZFP-insulin to IR485. We hence conclude the decreases in affinity for insulin of (i) the IRΔ703 construct upon mutation of this residue to alanine (*13*), (ii) the IR468/IR αCT.714A peptide mix (*17*), and (iii) the IR485 construct/IR αCT.714A peptide mix all result from the loss of a wild-type interaction between the IR Phe714 side chain and insulin rather than from a loss of interaction between the αCT peptide and the receptor. The nature of the IR Phe714−insulin interaction is not yet understood but may involve interaction with the insulin B-chain C-terminus when it is displaced from the insulin core on ligand binding (*22*).

Our ITC studies underscore the crucial role of the IR αCT peptide in the binding of insulin to its receptor. The demonstration here of a direct interaction between the αCT peptide and the first three domains of the insulin receptor lends strong support to the view that the segment of electron density lying on the face of the central β-sheet of the L1 domains in the crystal structure of the apo form of the IR ectodomain indeed arises from the IR αCT peptide in ligand binding. The similarity of the Site 1 mimetic peptides with the IR αCT peptide adds a further perspective to the role of the αCT peptide. Details of these interactions await three-dimensional structures of the receptor ectodomain or fragments thereof in complex with insulin; such studies are actively underway in our laboratory.

ACKNOWLEDGMENT

We thank Professor Ray Norton and Dr. Charles Galea (WEHI) for providing us with unpublished NMR data obtained from the IR αCT peptide in solution. We also thank Drs. Neil McKern, George Lovrecz, and Louis Lu (CSIRO) for advice during the protein expression and purification stages of this work.

REFERENCES

1. Adams, T. E., Epa, V. C., Garrett, T. P., and Ward, C. W. (2000) Structure and function of the type 1 insulin-like growth factor receptor. *Cell. Mol. Life Sci.57*, 1050–1093.
2. De Meyts, P. (1994) The structural basis of insulin and insulin-like growth factor-I receptor binding and negative co-operativity, and its relevance to mitogenic versus metabolic signalling. *Diabetologia37*/ (Suppl. 2), S135–S148.
3. De Meyts, P., and Whittaker, J. (2002) Structural biology of insulin and IGF1 receptors: Implications for drug design. *Nat. Rev. Drug Discovery1*, 769–783.
4. McKern, N. M., Lawrence, M. C., Streltsov, V. A., Lou, M. Z., Adams, T. E., Lovrecz, G. O., Elleman, T. C., Richards, K. M., Bentley, J. D., Pilling, P. A., Hoyne, P. A., Cartledge, K. A., Pham, T. M., Lewis, J. L., Sankovich, S. E., Stoichevska, V., Da Silva, E., Robinson, C. P., Frenkel, M. J., Sparrow, L. G., Fernley, R. T., Epa, V. C., and Ward, C. W. (2006) Structure of the insulin receptor ectodomain reveals a folded-over conformation. *Nature443*, 218–221.
5. Sparrow, L. G., Lawrence, M. C., Gorman, J. J., Strike, P. M., Robinson, C. P., McKern, N. M., and Ward, C. W. (2007) N-Linked glycans of the human insulin receptor and their distribution over the crystal structure. *Proteins: Struct., Funct., Bioinf.71*, 426–439.
6. Lou, M., Garrett, T. P., McKern, N. M., Hoyne, P. A., Epa, V. C., Bentley, J. D., Lovrecz, G. O., Cosgrove, L. J., Frenkel, M. J., and Ward, C. W. (2006) The first three domains of the insulin receptor differ structurally from the insulin-like growth factor 1 receptor in the regions governing ligand specificity. *Proc. Natl. Acad. Sci. U.S.A.103*, 12429–12434.

7. Zhang, B., and Roth, R. A. (1991) Binding properties of chimeric insulin receptors containing the cysteine-rich domain of either the insulin-like growth factor I receptor or the insulin receptor related receptor. *Biochemistry30*, 5113–5117.
8. Schumacher, R., Mosthaf, L., Schlessinger, J., Brandenburg, D., and Ullrich, A. (1991) Insulin and insulin-like growth factor-1 binding specificity is determined by distinct regions of their cognate receptors. *J. Biol. Chem.266*, 19288–19295.
9. Schumacher, R., Soos, M. A., Schlessinger, J., Brandenburg, D., Siddle, K., and Ullrich, A. (1993) Signaling-competent receptor chimeras allow mapping of major insulin receptor binding domain determinants. *J. Biol. Chem.268*, 1087–1094.
10. Whittaker, L., Hao, C., Fu, W., and Whittaker, J. (2008) High-Affinity Insulin Binding: Insulin Interacts with Two Receptor Ligand Binding Sites. *Biochemistry47*, 12900–12909.
11. Lawrence, M. C., McKern, N. M., and Ward, C. W. (2007) Insulin receptor structure and its implications for the IGF-1 receptor. *Curr. Opin. Struct. Biol.17*, 699–705.
12. Kurose, T., Pashmforoush, M., Yoshimasa, Y., Carroll, R., Schwartz, G. P., Burke, G. T., Katsoyannis, P. G., and Steiner, D. F. (1994) Cross-linking of a B25 azidophenylalanine insulin derivative to the carboxyl-terminal region of the α-subunit of the insulin receptor. Identification of a new insulin-binding domain in the insulin receptor. *J. Biol. Chem.269*, 29190–29197.
13. Mynarcik, D. C., Yu, G. Q., and Whittaker, J. (1996) Alanine-scanning mutagenesis of a C-terminal ligand binding domain of the insulin receptor α subunit. *J. Biol. Chem.271*, 2439–2442.
14. Schaefer, E. M., Siddle, K., and Ellis, L. (1990) Deletion analysis of the human insulin receptor ectodomain reveals independently folded soluble subdomains and insulin binding by a monomeric α-subunit. *J. Biol. Chem.265*, 13248–13253.
15. Kristensen, C., Wiberg, F. C., Schäffer, L., and Andersen, A. S. (1998) Expression and characterization of a 70-kDa fragment of the insulin receptor that binds insulin. Minimizing ligand binding domain of the insulin receptor. *J. Biol. Chem.273*, 17780–17786.
16. Kristensen, C., Wiberg, F. C., and Andersen, A. S. (1999) Specificity of insulin and insulin-like growth factor I receptors investigated using chimeric mini-receptors. Role of C-terminal of receptor α subunit. *J. Biol. Chem.274*, 37351–37356.
17. Kristensen, C., Andersen, A. S., Østergaard, S., Hansen, P. H., and Brandt, J. (2002) Functional reconstitution of insulin receptor binding site from non-binding receptor fragments. *J. Biol. Chem.277*, 18340–18345.
18. Huang, K., Chan, S. J., Hua, Q. X., Chu, Y. C., Wang, R. Y., Klaproth, B., Jia, W., Whittaker, J., De Meyts, P., Nakagawa, S. H., Steiner, D. F., Katsoyannis, P. G., and Weiss, M. A. (2007) The A-chain of insulin contacts the insert domain of the insulin receptor. Photo-cross-linking and mutagenesis of a diabetes-related crevice. *J. Biol. Chem.282*, 35337–35349.
19. Wan, Z., Xu, B., Huang, K., Chu, Y. C., Li, B., Nakagawa, S. H., Qu, Y., Hu, S. Q., Katsoyannis, P. G., and Weiss, M. A. (2004) Enhancing the activity of insulin at the receptor interface: Crystal structure and photo-cross-linking of A8 analogues. *Biochemistry43*, 16119–16133.
20. Schäffer, L., Brissette, R. E., Spetzler, J. C., Pillutla, R. C., Østergaard, S., Lennick, M., Brandt, J., Fletcher, P. W., Danielsen, G. M., Hsiao, K. C., Andersen, A. S., Dedova, O., Ribel, U., Hoeg-Jensen, T., Hansen, P. H., Blume, A. J., Markussen, J., and Goldstein, N. I. (2003) Assembly of high-affinity insulin receptor agonists and antagonists from peptide building blocks. *Proc. Natl. Acad. Sci. U. S.A.100*, 4435–4439.
21. Pillutla, R. C., Hsiao, K. C., Beasley, J. R., Brandt, J., Østergaard, S., Hansen, P. H., Spetzler, J. C., Danielsen, G. M., Andersen, A. S., Brissette, R. E., Lennick, M., Fletcher, P. W., Blume, A. J., Schäffer, L., and Goldstein, N. I. (2002) Peptides identify the critical hotspots involved in the biological activation of the insulin receptor. *J. Biol. Chem.277*, 22590–22594.
22. Ward, C. W., and Lawrence, M. C. (2009) Ligand-induced activation of the insulin receptor: A multi-step process involving structural changes in both the ligand and the receptor. *BioEssays31*, 422–434.
23. Ellman, G. L. (1958) A colorimetric method for determining low concentrations of mercaptans. *Arch. Biochem. Biophys.74*, 443–450.
24. Eyer, P., Worek, F., Kiderlen, D., Sinko, G., Stuglin, A., Simeon-Rudolf, V., and Reiner, E. (2003) Molar absorption coefficients for the reduced Ellman reagent: Reassessment. *Anal. Biochem.312*, 224–227.
25. Wiseman, T., Williston, S., Brandts, J. F., and Lin, L. N. (1989) Rapid measurement of binding constants and heats of binding using a new titration calorimeter. *Anal. Biochem.179*, 131–137.
26. Turnbull, W. B., and Daranas, A. H. (2003) On the value of c: Can low affinity systems be studied by isothermal titration calorimetry?. *J. Am. Chem. Soc.125*, 14859–14866.
27. Tellinghuisen, J. (2008) Isothermal titration calorimetry at very low c. *Anal. Biochem.373*, 395–397.
28. Mynarcik, D. C., Williams, P. F., Schäffer, L., Yu, G. Q., and Whittaker, J. (1997) Identification of common ligand binding determinants of the insulin and insulin-like growth factor 1 receptors. Insights into mechanisms of ligand binding. *J. Biol. Chem.272*, 18650–18655.